DOI: 10.1002/ejic.200800175

Synthesis, Characterization, and Magnetic Properties of a 1D Oxalate-Bridged Mn^{II} Complex Consisting of 10-Membered Ring Units

Wei Li,[a] Hong-Peng Jia,[a] Zhan-Feng Ju,[a] and Jie Zhang*[a]

Keywords: Magnetic properties / Spin-canting / Oxalate complexes / Manganese / Bipyridinium

Self-assembly of the newly synthesized 2-methyl-4,6-bis(4′-pyridyl-1′-pyridinio)pyrimidine dichloride ($MbppCl_2$) with $MnCl_2{\cdot}4H_2O$ and $Na_2C_2O_4$ affords an unprecedented chain-like oxalate-bridged Mn^{II} polymer consisting of 10-membered ring units, $\{[Mn_3(OH)(H_2O)_2(Mbpp)(C_2O_4)_{3.5}]{\cdot}6.5H_2O\}_n$ (**1**), which exhibits spin-canted antiferromagnetism at low temperature.

Introduction

Oxalate-bridged complexes have attracted intense interest in the field of molecule-based magnetic materials because they can mediate strong magnetic interactions between different paramagnetic centers separated by more than 5 Å to form diverse phases which exhibit ferro-, ferri-, or canted antiferromagnetic ordering.[1–5] A plethora of oxalate-bridged magnetic systems have been well characterized, accompanied by considerable magnetostructural studies from both experimental and theoretical viewpoints. The strong coordination tendency with transition metals and the various bridging abilities of the oxalate anion provide numerous advantages for constructing homometallic or heterometallic magnetic architectures with various structural characteristics, and it is possible to control the steric arrangement of oxalate-bridged complexes by the suitable choice of the cationic templates or capping organic ligands.[6] For the reported oxalate-bridged coordination polymers, the 3D 10-gon 3-connected (10,3) anionic network,[7] the 2D honeycomb systems,[8] and 1D zigzag or linear chain structures are frequently present,[4,9] whereas the 1D chain structures built by ring-like units are quite rare; only a few examples with four-membered ring units are known to date.[10] The studies on magnetostructural correlations revealed that some 3D oxalate-bridged complexes behaving as ferro- or ferrimagnets exhibit lower ordering temperatures than their 2D analogues,[6b,11] thus the 1D oxalate complexes with analogous ring-like units are of special interest for magnetic studies. In this paper, we synthesized a new bipyridinium salt, 2-methyl-4,6-bis(4′-pyridyl-1′-pyridinio)pyrimidine dichloride ($MbppCl_2$). The self-assembly of $MbppCl_2$ with $MnCl_2{\cdot}4H_2O$ and $Na_2C_2O_4$ afforded an unprecedented 1D oxalate-bridged Mn^{II} polymer consisting of 10-membered ring units, $\{[Mn_3(OH)(H_2O)_2(Mbpp)(C_2O_4)_{3.5}]{\cdot}6.5H_2O\}_n$ (**1**). It is interesting that spin-canted antiferromagnetism was observed at low temperature for **1**.

Results and Discussion

X-ray Crystal Structure of $\{[Mn_3(OH)(H_2O)_2(Mbpp)(C_2O_4)_{3.5}]{\cdot}6.5H_2O\}_n$ (1)

A single-crystal X-ray diffraction study revealed that the asymmetric unit of complex **1** has three crystallographically independent Mn^{II} ions, a $Mbpp^{2+}$ cation, three and a half oxalate anions, one hydroxide anion, two coordinated water molecules, and six and a half solvent water molecules (Figure 1). All Mn^{II} ions are surrounded by chiral octahedral coordination spheres (Λ configuration in the measurement crystal). Mn1 is coordinated side-on by three bischelating oxalate ligands. Mn2 is coordinated by two bischelating oxalate groups, a terminal nitrogen atom from the $Mbpp^{2+}$ ligand and one oxygen atom from a water molecule or a hydroxide group. Mn3 has an octahedral geometry defined by six oxygen atoms: four from two chelating oxalate groups, two from two water molecules or a water molecule and a hydroxide group. The position of the hydroxide group is hard to fix based on the present X-ray diffraction data. The Mn–O and Mn–N bond lengths are in the range of 2.143–2.327 Å, and the O–Mn–O and N–Mn–O bite angles vary from 74.33 to 105.70°, which are comparable to the observed values in Mn^{II} complexes containing bridging oxalate groups and coordinated pyridine ligands.[12] Interestingly, Mn1, Mn2, and Mn3 ions are connected by bischelating oxalate bridges to form a 10-membered Mn3–Mn1–Mn2–Mn1A–Mn3A–Mn3C–Mn1C–Mn2B–Mn1B–Mn3B–Mn3 ring, which is further linked into a 1D

[a] State Key Laboratory of Structural Chemistry, Fujian Institute of Research on the Structure of Matter, The Chinese Academy of Sciences,
Fuzhou, Fujian 350002, China
Fax: +86-591-83710051
E-mail: zhangjie@fjirsm.ac.cn

Supporting information for this article is available on the WWW under http://www.eurjic.org or from the author.

loop chain along the *b* axis by sharing Mn1–Mn3–Mn3–Mn1 moieties (Figure 2, a). In the 10-membered ring, all metal ions show the same chirality, consequently leading to the formation of a homochiral loop chain. For oxalate-bridged complexes, the ring-like subunits are common structural motifs within 2D and 3D coordination networks; the presence of one or both $[M(ox)_3]^{3-}$ enantiomers plays an important role in the dimensionality of the polymetallic systems.[10b] The alternating arrangement of Δ and Λ configurations of $[M(ox)_3]^{3-}$ give rise to a 2D (6,3) honeycomb layer. If adjacent bridged metal centers have the same chirality, the resulting network is a 3D (10,3) topology. The ring-like subunits are rarely present within the 1D polymers; only two examples with four-membered ring units have been reported until now.[10] It is interesting to note that all of these loop chains are chiral although the chiral templating cations, which are thought to be a determining factor in the formation of 3D chiral frameworks,[13] are not introduced.

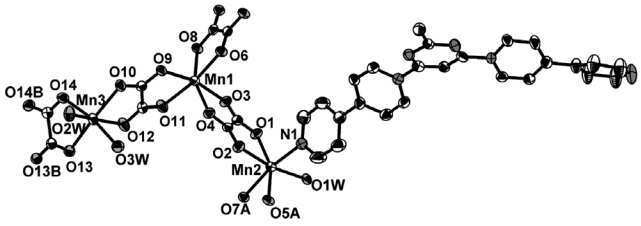

Figure 1. The molecular structure of complex **1** with thermal ellipsoids drawn at the 50% probability level. Free water molecules and all hydrogen atoms have been omitted for clarity. Symmetry codes: A: *x*, *y* – 1, *z*; B: –*x*, *y*, 0.5 – *z*.

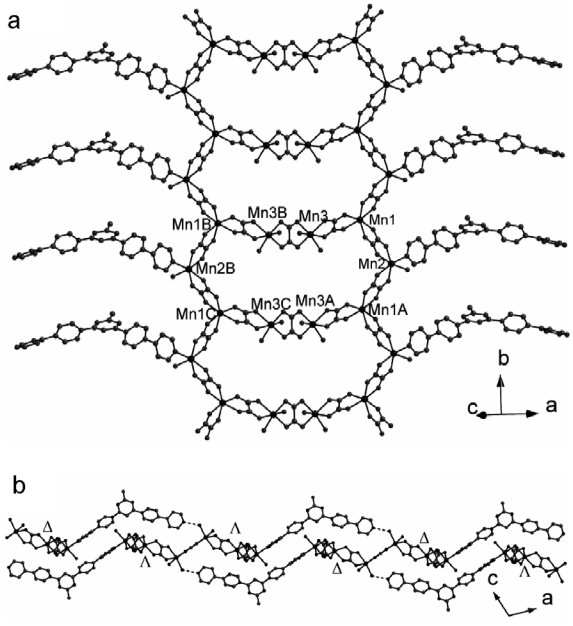

Figure 2. (a) The 1D millipede-like chain structure containing 10-membered ring units in complex **1**. (b) The 2D layer-like structure constructed from hydrogen bonds in **1**, viewed along the *b*-axis direction. Free water molecules and all hydrogen atoms have been omitted for clarity. The dashed lines represent hydrogen bonds. Symmetry codes: A: *x*, *y* – 1, *z*; B: –*x*, *y*, 0.5 – *z*; C: –*x*, *y* – 1, 0.5 – *z*.

In the structure of **1**, each $Mbpp^{2+}$ cation is nonplanar. The interplanar angles between the adjacent pyridyl rings are ca. 39°, while those between the pyrimidine ring and its adjoining pyridyl rings are 18.5 and 36.6°. It is worth mentioning that the cationic $Mbpp^{2+}$ ligand utilizes only one of the terminal nitrogen atoms (N1) to coordinate with a Mn^{II} ion, leading to the generation of a millipede-like chain (Figure 2, a). The interchain hydrogen-bonding interaction between another terminal nitrogen atom (N6) and the coordinated O2W atom joins the 1D millipede-like chain together into a 2D supramolecular network, in which adjacent chains exhibit opposite chirality, and thus the whole 2D layer is achiral (Figure 2, b). The kidney-shaped ring unit in **1** is longer and narrower than the reported ten-numbered ring in the 3D (10,3) topologies.[7] The long V-type $Mbpp^{2+}$ ligand might play a role in manipulating this kind of shape. As viewed from Figure 2 (b), the crankle of the Mn^{II} ring configuration suits the V-type structure of the $Mbpp^{2+}$ ligand.

Magnetic Properties

The magnetic property of complex **1** in the form of the χ_m and $\chi_m T$ product against T plots [χ_m being the magnetic susceptibility per mol of Mn_3 unit] is shown in Figure 3. The $\chi_m T$ value at room temperature is 11.71 emu K mol^{-1}, a value slightly lower than that expected for three isolated Mn^{II} ions (13.125 emu K mol^{-1} for S = 5/2 with g = 2.0). As the temperature is lowered from 300 to 50 K, there is a smooth decrease in the $\chi_m T$ value, whereas below 50 K, the $\chi_m T$ value sharply decreases and reaches 0.90 emu K mol^{-1} at 2 K. This is the obvious character of antiferromagnetic

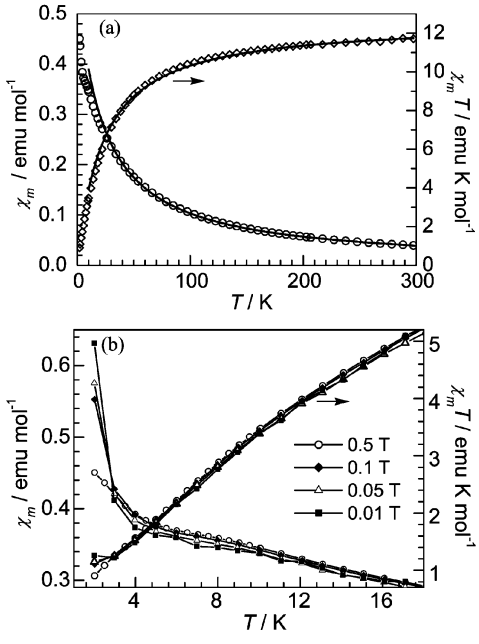

Figure 3. (a) Temperature dependence of the χ_m and $\chi_m T$ product for complex **1**, H = 0.5 T. The solid lines correspond to the Curie–Weiss fit. (b) Temperature dependence of the χ_m and $\chi_m T$ product under different applied fields for complex **1**.

interaction, and the data above 10 K can be well described by a Curie–Weiss law with C = 12.6 emu K mol^{-1} and θ = –22.3 K. Below 3 K and at a low applied field of 0.01 T, the $\chi_m T$ product experiences an upturn, arriving at 1.18 emu K mol^{-1} at 2 K. When an applied field is larger than 0.01 T, the upturn of $\chi_m T$ product becomes unconspicuous and completely disappears at higher field (>0.05 T). Upon cooling, the χ_m value is smoothly raised and undergoes an inflection around 6.5 K. Below the inflection temperature, a relatively abrupt increase, which is more obvious in lower magnetic fields, can be observed. This low temperature behavior suggests the occurrence of very weak ferromagnetic interactions in complex **1**, which may arise from the presence of canting between the antiparallel alignment of the spins.[14]

The zero-field ac magnetic susceptibility measurements show a slow increase upon cooling with a small plateau around 6.2 K and a rapid rise below 2.8 K in the in-phase signal (χ_m') versus T plot. The appearance of a nonzero out-of-phase (χ_m'') signal below 2.2 K confirms the presence of a ferromagnetically ordered state (Figure 4). No visible maximum suggests that the ferromagnetic ordering temperature should be lower than 2 K. The field-dependent isothermal magnetization at 2 K increases linearly with increasing field in the high-field region (Figure 5). The magnetization is far from saturation up to the highest applied field of 7 T, reaching a maximum value of 4.32 $N\beta$ that is much lower than the expected saturation value of 15 $N\beta$ for

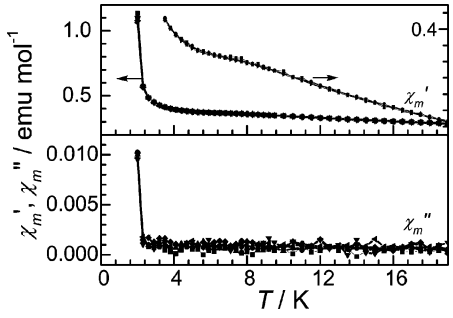

Figure 4. The in-phase χ_m' and out-of phase χ_m'' signals of ac susceptibilities as a function of temperature at a zero dc field and an ac field of 3 Oe with different frequencies ranging from 111 to 3511 Hz.

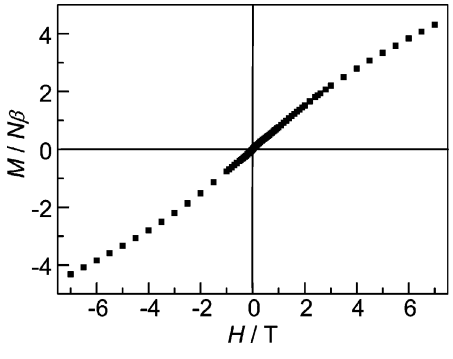

Figure 5. The isothermal magnetization curves for complex **1** at 2 K in the applied field range 0–7 T.

three isolated Mn^{II} species (S = 5/2). This observation is consistent with a canted antiferromagnetic state. No magnetic hysteresis was found at 2 K.

It is well known that the occurrence of spin canting is usually caused by either single-ion magnetic anisotropy or antisymmetric Dzyaloshinsky–Moriya exchange in magnetic entities.[15] Because of the negligible single-ion anisotropy for high-spin Mn^{II},[14] the spin-canted phenomenon observed for **1** at low temperatures should arise from the antisymmetric exchange. Although **1** crystallizes in a centrosymmetric $C2/c$ space group, the magnetic structure is acentric as a sublattice. The coordination environments around adjacent Mn3 and Mn1, Mn1 and Mn2, Mn2 and Mn1A are completely different, and all the Mn^{II} ions within the 1D chain have the same chirality; there are no inversion centers between two magnetic sites. Thus the antisymmetric exchange between neighboring Mn^{II} ions is possible and results in the observed spin-canting phenomenon.[16]

Characterization and Analysis of IR Spectra

The FTIR spectrum of $MbppCl_2$ exhibits sharp bands at 1640 and 1610 cm^{-1} due to the typical C=N and C=C stretching vibrations arising from pyridinium and pyridyl rings. In the spectrum of complex **1**, these characteristic C=N and C=C vibration bands are superimposed on the ν_{as}(COO) stretching vibrations of the oxalate anion, showing a broad band in the 1683–1610 cm^{-1} region. The absorption peaks centered at 1683 and 1664 [ν_{as}(COO)], 1311 [ν_s(COO)], and 790 cm^{-1} [δ(OCO)] are consistent with the presence of the tetradentate oxalate-bridged group.[17] The appearance of two ν_{as}(COO) vibrations can be attributed to the shorter C=O bond length (1683 cm^{-1}) and the longer C=O (1664 cm^{-1}) in the oxalate-bridged complex **1**.[18]

Conclusions

In conclusion, by utilizing a newly synthesized bipyridinium salt ($MbppCl_2$) in assembly with $MnCl_2{\cdot}4H_2O$ and $Na_2C_2O_4$ in aqueous solution, an unprecedented chain-like oxalate-bridged Mn^{II} polymer consisting of 10-membered ring units $\{[Mn_3(OH)(H_2O)_2(Mbpp)(C_2O_4)_{3.5}]{\cdot}6.5H_2O\}_n$ was successfully synthesized and structurally characterized. The spin-canted antiferromagnetism was observed at low temperature.

Experimental Section

General Remarks: All chemicals were of reagent grade and were used without further purification. IR spectra were recorded with a Spectrum One FTIR spectrophotometer on KBr pellets in the range 4000–400 cm^{-1}. Elemental analyses were performed using a Vario EL III CHNOS elemental analyzer. ^{1}H NMR spectra were recorded with a Varian Unity 500 NMR spectrometer operating at 500 MHz in D_2O. Variable-temperature magnetic susceptibility measurements were preformed using a Quantum Design PPMS-9T system. All data were corrected for diamagnetism of the samples estimated from Pascal's constants.

Preparation of 2-Methyl-4,6-bis(4′-pyridyl-1′-pyridinio)pyrimidine Dichloride ($MbppCl_2$): A mixture of 4,4′-bipyridine (50 mmol, 7.18 g) and 4,6-dichloro-2-methylpyrimidine (20 mmol, 3.26 g) was dissolved in dmf (30 mL) and then stirred at 50 °C under nitrogen for 12 h. After the mixture was cooled to room temp., the resulting precipitate was filtered off, washed with a small amount of dmf and dried to give $MbppCl_2$ as a green powder. Yield: 5.28 g, 55%. FTIR (KBr): $\tilde{\nu}$ = 3073 (w), 3022 (w), 1640 (vs), 1610 (vs), 1591 (sh), 1576 (vs), 1565 (vs), 1538 (sh), 1490 (w), 1445 (w), 1411 (vs), 1364 (m), 1340 (w), 1293 (w), 1221 (s), 1149 (m), 1126 (w), 1107 (w), 1037 (w), 995 (m), 820 (vs), 746 (s), 719 (m), 613 (w) cm^{-1}. ^1H NMR (400 MHz, D_2O): δ = 9.94 (d, 4 H), 9.05 (s, 1 H), 8.91 (d, 4 H), 8.85 (d, 4 H), 8.14 (d, 4 H), 3.14 (s, 3 H) ppm.

$\{[Mn_3(OH)(H_2O)_2(Mbpp)(C_2O_4)_{3.5}]\cdot 6.5H_2O\}_n$ (1): Light-brown sheet crystals of complex **1** were obtained at room temp. in the darkness by a slow layering of a water solution (3 mL) of $MnCl_2\cdot 4H_2O$ (0.1 mmol, 0.020 g) into a water/dmso (1:5) solution (3 mL) of $MbppCl_2$ (0.1 mmol, 0.048 g) and $Na_2C_2O_4$ (0.1 mmol, 0.013 g). Yield: 0.055 g, 52% based on manganese. $C_{32}H_{38}Mn_3N_6O_{23.5}$ (1047.50): calcd. C 36.38, H 3.72, N 7.95; found C 36.29, H 3.54, N 8.30. FTIR (KBr): $\tilde{\nu}$ = 3412 (b), 3126 (w), 3058 (w), 1683 (sh), 1664 (m), 1618 (vs), 1610 (vs), 1411 (w), 1366 (w), 1311 (m), 1217 (w), 1137 (w), 1015 (w), 790 (m), 753 (w), 497 (w), 444 (w) cm^{-1}.

X-ray Crystallographic Studies: Data collection was performed using a Rigaku Mercury CCD diffractometer with graphite-monochromated Mo-K_α radiation (λ = 0.71073 Å) at 293(2) K. The structures were solved by direct methods and refined by full-matrix least-squares on F^2 using the SHELXL-97 program package.[19] All non-hydrogen atoms were refined anisotropically, and the hydrogen atoms bonded to carbon atoms were positioned geometrically and refined using a riding model. No chloride expected as counteranion was found in the crystal structure; there is a hydroxide anion among the coordinated water molecules. Selected bond lengths and angles are listed in Table 1. Crystallographic data and other pertinent information for complex **1** are summarized in Table 2.

Table 1. Selected bond lengths [Å] and angles [°] for **1**.[a]

Mn1–O3	2.195(4)	Mn2–O1	2.170(4)
Mn1–O4	2.198(4)	Mn2–O2	2.240(4)
Mn1–O6	2.164(4)	Mn2–O5A	2.143(4)
Mn1–O8	2.183(4)	Mn2–O7A	2.277(4)
Mn1–O9	2.144(4)	Mn2–O1W	2.327(4)
Mn1–O11	2.177(5)	Mn2–N1	2.254(6)
Mn3–O10	2.176(4)	Mn3–O14	2.191(5)
Mn3–O12	2.188(5)	Mn3–O2W	2.154(5)
Mn3–O13	2.171(5)	Mn3–O3W	2.267(5)
O3–Mn1–O4	75.52(16)	O1–Mn2–N1	97.8(2)
O3–Mn1–O6	96.67(18)	O1–Mn2–O2	74.33(16)
O3–Mn1–O8	86.59(16)	O1–Mn2–O7A	92.38(17)
O3–Mn1–O11	93.94(18)	O1–Mn2–O1W	97.13(15)
O4–Mn1–O6	92.51(17)	O2–Mn2–O5A	87.71(17)
O4–Mn1–O9	94.07(18)	O2–Mn2–O7A	97.12(17)
O4–Mn1–O11	90.52(19)	O2–Mn2–N1	88.1(2)
O6–Mn1–O8	75.71(15)	O5A–Mn2–O7A	75.23(15)
O6–Mn1–O9	93.56(17)	O5A–Mn2–N1	95.9(2)
O8–Mn1–O9	105.70(18)	O7A–Mn2–O1W	90.23(15)
O8–Mn1–O11	104.61(17)	N1–Mn2–O1W	86.05(19)
O9–Mn1–O11	76.06(17)	O3W–Mn3–O10	92.00(19)
O2W–Mn3–O10	97.40(19)	O3W–Mn3–O12	87.1(2)
O2W–Mn3–O13	98.5(2)	O3W–Mn3–O13	95.87(17)
O2W–Mn3–O14	92.2(2)	O10–Mn3–O12	75.85(17)
O2W–Mn3–O3W	83.52(19)	O10–Mn3–O14	97.71(18)
O12–Mn3–O13	89.41(18)	O13–Mn3–O14	75.57(17)
O12–Mn3–O14	98.1(2)		

[a] Symmetry codes: A: x, $y-1$, z.

Table 2. Crystallographic data for complex **1**.

Empirical formula	$C_{32}H_{38}Mn_3N_6O_{23.5}$
Formula weight	1047.50
Crystal size [mm]	0.40 × 0.30 × 0.20
Crystal system	monoclinic
Space group	*C*2/*c*
a [Å]	52.64(2)
b [Å]	9.406(4)
c [Å]	18.316(7)
β [°]	109.263(9)
Volume [Å^3]	8562(6)
Z	8
$D_{calcd.}$ [g cm^{-3}]	1.625
Absorption coefficient [mm^{-1}]	0.966
F(000)	4280
Temperature [K]	293(2)
Reflections measured	32461
Independent reflections	9745 [*R*(int) = 0.0799]
R_1, wR_2 [$I > 2\sigma(I)$]	0.0922, 0.2181
R_1, wR_2 (all data)	0.1534, 0.2610
Goodness-of-fit	1.072

CCDC-677677 contains the supplementary crystallographic data for compound **1**. These data can be obtained free of charge from The Cambridge Crystallographic Data Centre via www.ccdc.cam.ac.uk/data_request/cif.

Supporting Information (see also the footnote on the first page of this article): IR spectra of $MbppCl_2$ and complex **1**.

Acknowledgments

The authors acknowledge the financial support of the Chinese National Natural Science Foundation (No.20671090/50372069), the Chinese Natural Science Foundation of Fujian Province (No. E0220003), and Key Project from CAS (KJCX2.YW.H01).

[1] J. S. Miller, M. Drillon (Eds.), *Magnetism: Molecules to Materials II*, Wiley-VCH, Weinheim, **2001**.
[2] H. Tamaki, Z. J. Zhong, N. Matsumoto, S. Kida, M. Koikawa, N. Achiwa, Y. Hashimoto, H. Okawa, *J. Am. Chem. Soc.* **1992**, *114*, 6974–6979.
[3] D. Armentano, G. De Munno, T. F. Mastropietro, D. M. Proserpio, M. Julve, F. Lloret, *Inorg. Chem.* **2004**, *43*, 5177–5179.
[4] C. N. R. Rao, S. Natarajan, R. Vaidhyanathan, *Angew. Chem. Int. Ed.* **2004**, *43*, 1466–1496.
[5] H.-B. Xu, Z.-M. Wang, T. Liu, S. Gao, *Inorg. Chem.* **2007**, *46*, 3089–3096.
[6] a) J. J. Novoa, D. Braga, L. Addadi (Eds.), *Engineering of Crystalline Materials Properties*, Springer, **2008**, pp. 173–191; b) E. Coronado, J. R. Galán-Mascarós, C. Martí-Gastaldo, *Polyhedron* **2007**, *26*, 2101–2104.
[7] a) S. Decurtins, H. W. Schmalle, P. Schneuwly, H. R. Oswald, *Inorg. Chem.* **1993**, *32*, 1888–1892; b) S. Decurtins, H. W. Schmalle, P. Schneuwly, J. Ensling, P. Gütlich, *J. Am. Chem. Soc.* **1994**, *116*, 9521–9528; c) E. Coronado, J. R. Galán-Mascarós, C. J. Gómez-García, J. M. Martínez-Agudo, *Inorg. Chem.* **2001**, *40*, 113–120; d) E. Coronado, J. R. Galán-Mascarós, M. C. Giménez-López, M. Almeida, J. C. Waerenborgh, *Polyhedron* **2007**, *26*, 1838–1844, and references therein.
[8] a) R. Pellaux, H. W. Schmalle, R. Huber, P. Fischer, T. Hauss, B. Ouladdiaf, S. Decurtins, *Inorg. Chem.* **1997**, *36*, 2301–2308; b) A. Alberola, E. Coronado, J. R. Galán-Mascarós, C. Gimé-

nez-Saiz, C. J. Gómez-García, *J. Am. Chem. Soc.* **2003**, *125*, 10774–10775; c) E. Coronado, J. R. Galán-Mascarós, C. Martí-Gastaldo, A. M. Martínez, *Dalton Trans.* **2006**, 3294–3299.

[9] a) H. Oshio, U. Nagashima, *Inorg. Chem.* **1992**, *31*, 3295–3301; b) J. P. García-Terán, O. Castillo, A. Luque, U. García-Couceiro, G. Beobide, P. Román, *Dalton. Trans.* **2006**, 902–911; c) L.-L. Li, K.-J. Lin, C.-J. Ho, C.-P. Sun, H.-D. Yang, *Chem. Commun.* **2006**, 1286–1288; d) S. Kitagawa, T. Okubo, S. Kawata, M. Kondo, M. Katada, H. Kobayashi, *Inorg. Chem.* **1995**, *34*, 4790–4796; e) U. García-Couceiro, O. Castillo, A. Luque, J. P. García-Terán, G. Beobide, P. Román, *Eur. J. Inorg. Chem.* **2005**, 4280–4290.

[10] a) E. Cariati, R. Macchi, D. Roberto, R. Ugo, S. Galli, N. Casati, P. Macchi, A. Sironi, L. Bogani, A. Caneschi, D. Gatteschi, *J. Am. Chem. Soc.* **2007**, *129*, 9410–9420; b) F. D. Rochon, R. Melanson, M. Andruh, *Inorg. Chem.* **1996**, *35*, 6086–6092.

[11] E. Coronado, J. R. Galán-Mascarós, C. J. Gómez-García, E. Martínez-Ferrero, M. Almeida, J. C. Waerenborgh, *Eur. J. Inorg. Chem.* **2005**, 2064–2070.

[12] a) E. Yang, X.-Q. Wang, S.-Y. Chen, *Chin. J. Struct. Chem.* **2006**, *25*, 873–977; b) U. Garcia-Couceiro, O. Castillo, A. Luque, J. P. Garcia-Teran, G. Beobide, P. Roman, *Cryst. Growth Des.* **2006**, *6*, 1839–1847.

[13] R. Andrés, M. Brissard, M. Gruselle, C. Train, J. Vaissermann, B. Malézieux, J. P. Jamet, M. Verdaguer, *Inorg. Chem.* **2001**, *40*, 4633–4640.

[14] R. L. Carlin, *Magnetochemistry*, Springer-Verlag, Berlin, Heidelberg, **1986**.

[15] O. Castillo, A. Luque, P. Román, F. Lloret, M. Julve, *Inorg. Chem.* **2001**, *40*, 5526–5535, and references therein.

[16] E.-Q. Gao, Y.-F. Yue, S.-Q. Bai, Z. He, S.-W. Zhang, C.-H. Yan, *Chem. Mater.* **2004**, *16*, 1590–1596.

[17] a) T. Fujino, Y. Hoshino, S. Igarashi, Y. Masuda, Y. Yukawa, *Inorg. Chim. Acta* **2004**, *357*, 11–18; b) L. P. Battaglia, A. Bianchi, A. B. Corradi, E. Garcia-España, M. Micheloni, M. Julve, *Inorg. Chem.* **1988**, *27*, 4174–4179.

[18] C. S. Hong, J. H. Yoon, Y. S. You, *Inorg. Chem. Commun.* **2005**, *8*, 310–313.

[19] G. M. Sheldrick, *SHELXL-97: Program for the Refinement of Crystal Structures*, University of Göttingen, Göttingen, Germany, **1997**.

Received: February 15, 2008
Published Online: June 6, 2008

